PCCP

RSC Publishing

PAPER

View Article Online
View Journal | View Issue

Cite this: *Phys. Chem. Chem. Phys.*, 2013, **15**, 15477

Cu_3MCh_3 (M = Sb, Bi; Ch = S, Se) as candidate solar cell absorbers: insights from theory

Aoife B. Kehoe,[a] Douglas J. Temple,[a] Graeme W. Watson*[a] and David O. Scanlon*[b]

Received 14th June 2013,
Accepted 15th July 2013

DOI: 10.1039/c3cp52482e

www.rsc.org/pccp

As the thin film photovoltaic sector continues to expand, there is an emerging need to base these technologies on abundant, low cost materials in place of the expensive, rare, or toxic elements such as Te, In, or Cd that currently constitute the industry standards. To this end, the geometric and electronic structure of four materials comprising low cost, earth abundant elements (Cu_3SbS_3, Cu_3SbSe_3, Cu_3BiS_3, and Cu_3BiSe_3) are investigated with the screened hybrid exchange–correlation functional HSE06 and their candidacy for use as absorber materials assessed. The materials are shown to exhibit low VBM effective masses, due partially to the presence of lone pairs that originate from the Sb and Bi states. Although all four materials possess indirect fundamental band gaps, calculated optical absorbance shows direct transitions close in energy. Optical band gaps within the visible-light spectrum are also predicted for three of the systems, (Cu_3SbSe_3, Cu_3BiS_3 and Cu_3BiSe_3) making them promising candidates for PV applications.

1 Introduction

In an increasingly energy-dependent global society, the development of solar cell technologies that are sustainable, economically viable, and environmentally friendly is of paramount importance.[1] Ideal materials for solar cell absorbers are semiconductors with a direct optical band gap of around 1.5 eV and a high absorption coefficient of $\alpha \approx 10^5$ cm^{-1}.[2] In recent times, thin film photovoltaic (PV) semiconductor research has been dominated by CdTe and Cu(In,Ga)Se (CIGS),[3–6] which at 17.3% and 20.3%, respectively, have the highest efficiencies of any thin film solar cell absorbers.[7,8] However, these materials are not ideally suited to widespread application due to the toxicity of Cd and the scarcity of In and Te. In 2000 it was estimated that the availability of In and Te will limit the ultimate electricity-generating capacity of these materials to 4% of the current global demands for CdTe and 1% for CIGS.[9] Therefore, there is a pressing need to develop PV systems which are both environmentally sound and based on more abundant materials, such as Cu_2ZnSnS_4 (CZTS), $Cu_2ZnSnSe_4$ (CZTSe), $ZnSnP_2$, and Si_3AlP.[10–14]

Binary, ternary, and quaternary copper chalcogenide materials have been widely investigated as promising candidates for use in optoelectronic devices such as PV cells, optical recording media, and thermoelectrics.[15–22] In particular, CZTS and CZTSe have undergone widespread research as potential PV absorbers, comprising relatively inexpensive and non-toxic elements, possessing band gaps in the range 1.0–1.6 eV, and having reached efficiencies of 10.1%.[10,11,21,23–27]

The high availability and low cost of Sb and Bi makes compounds containing these elements, such as Sb_2Se_3,[28,29] Cu_3MCh_3 (M = Sb, Bi; Ch = S, Se),[19] and $CuMCh_2$ (M = Sb, Bi; Ch = S, Se),[20,30,31] worthy of investigation as alternatives to current PV materials. The US Geological Survey lists the global reserves of Sb and Bi at 1 800 000 and 320 000 tonnes, respectively, which are substantially more than the global reserves of Te (24 000 tonnes)[32] and In (estimated at 11 000 tonnes in 2008[33] and 2 800 tonnes in 2007[34]). In addition, Bi can be directly obtained from Bi ore, but lack of demand means that this method is typically not used over the indirect method of obtaining Bi as a by-product of lead refining.[35] Interestingly, a recent computational study by Yu *et al.* utilized an inverse design method to identify materials with a suitable solar absorption defined as the spectroscopic limited maximum efficiency (SLME), and identified Cu_x-V-VI_y materials as worthy of further investigation.[36] In this work we focus on the Cu_3-V-VI_3 family of materials, specifically Cu_3MCh_3 (M = Sb, Bi; Ch = S, Se).

There are three known temperature-dependent polymorphs of Cu_3SbS_3.[37] One is an orthorhombic structure analogous to Wittichenite (Fig. 1(a)) with lattice vectors $\boldsymbol{a}$ = 7.884 Å, $\boldsymbol{b}$ = 10.221 Å, and $\boldsymbol{c}$ = 6.624 Å[38] and space group $P2_12_12_1$. Each Sb is coordinated to three S ions in a pyramidal-like geometry. The Cu atoms are in a distorted trigonal planar coordination to three S atoms. There are two environments for S: a distorted

[a] *School of Chemistry and CRANN, Trinity College Dublin, Dublin 2, Ireland. E-mail: watsong@tcd.ie*

[b] *University College London, Kathleen Lonsdale Materials Chemistry, Department of Chemistry, 20 Gordon Street, London WC1H 0AJ, UK. E-mail: d.scanlon@ucl.ac.uk*

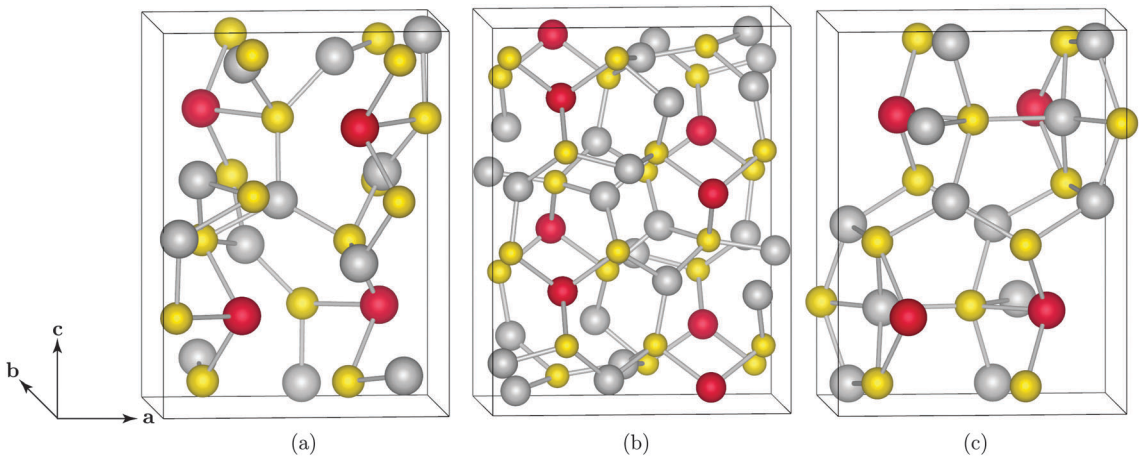

Fig. 1 Crystal structures of (a) Wittichenite, (b) Skinnerite, and (c) Cu_3SbSe_3. Cu atoms are shown as gray, Sb/Bi as red, and S/Se as yellow.

tetrahedral arrangement where the S is coordinated to one Sb and three Cu atoms, and a distorted trigonal planar structure with S coordinated to one Sb and two Cu atoms. Cu_3SbS_3 is stable in this form below 263 K, which was therefore used as the starting structure in this study because all calculations were performed at 0 K. Skinnerite (Fig. 1(b)) is a structure of space group $P2_1/c$ and lattice parameters $\boldsymbol{a}$ = 7.814 Å, $\boldsymbol{b}$ = 10.242 Å, and $\boldsymbol{c}$ = 13.273 Å.[39] It is adopted by Cu_3SbS_3 between 263 K and 395 K and consists of a small alternating distortion of the layers found in the low temperature structure. A third structure, an orthorhombic lattice with space group *Pnma* (Fig. 1(c)), exists at temperatures greater than 395 K. It contains Cu ions that have both three- and four-fold coordination to S, and Sb in trigonal pyramidal coordination to the anion. S exhibits five-fold coordination to four Cu and one Sb in a distorted trigonal bipyramidal geometry.

Cu_3SbSe_3 is isostructural to this third polymorph of Cu_3SbS_3 at room temperature, with lattice constants of $\boldsymbol{a}$ = 7.9865 Å, $\boldsymbol{b}$ = 10.6138 Å, $\boldsymbol{c}$ = 6.8372 Å.[40] Cu_3BiS_3 (Wittichenite) has the same structure as the low temperature phase of Cu_3SbS_3 with lattice vectors $\boldsymbol{a}$ = 7.723 Å, $\boldsymbol{b}$ = 10.395 Å, $\boldsymbol{c}$ = 6.716 Å.[41] No crystal structure data was found for Cu_3BiSe_3 so the structures of both Cu_3SbSe_3 and Wittichenite were tested as starting points for the optimization process, with the Cu_3SbSe_3 structure found to be 0.44 eV lower in energy than the Wittichenite structure and therefore used here. An additional justification for using the Cu_3SbSe_3 structure is that the two sulphide materials are isostructural at the simulation temperature, so the assumption that the two selenide structures are also isostructural is reasonable.

Of the four materials, Cu_3BiS_3 (Wittichenite) has been studied the most extensively.[42–46] It can be easily synthesized as thin films from starting materials that are relatively inexpensive and much less toxic than Cd. It is a p-type semiconductor with high optical absorbance in the visible region[42] and has a direct, forbidden, optical band gap of 1.4 eV.[44] Evidence of hole trapping has been observed, allowing for prolonged lifetime of electrons in the conduction band.[45] These properties make Cu_3BiS_3 thin films appear to be an appealing material for use as an absorber in PV cells.

Previous studies on low temperature Cu_3SbS_3 have mainly focused on nanorods[47] and nanowires of the Skinnerite phase, for which an indirect optical band gap of 2.95 eV was determined,[48] a value much too high for an efficient absorber material. Meanwhile, Cu_3SbSe_3 has been reported to display p-type conductivity and a direct optical band gap of 1.68 eV,[49] making it a potential absorber candidate. Cu_3BiSe_3 has yet to be considered as a potential solar cell absorber, with only one recent publication on the material, which examined the phases of Cu–Bi–Se systems.[50]

In this study, we explore the geometry, electronic structure and optical properties of the copper chalcogenide series, Cu_3MCh_3 (M = Sb, Bi; Ch = S, Se), using screened hybrid density functional theory (DFT) methods. We also consider the effect of the lone pairs on Sb and Bi on the electronic structure. From this, we discuss the potential suitability of these materials to applications as solar cell absorbers.

2 Computational methods

The systems were modeled using periodic DFT in the Vienna *ab initio* Simulation Package (VASP).[51,52] Calculations were performed with the screened hybrid density functional of Heyd, Scuseria, and Ernzerhof (HSE06).[53] HSE06 was chosen over other hybrid functionals such as B3LYP[54] or PBE0[55] as, unlike its alternatives, HSE06 is a screened functional. In the HSE06 method, the exchange–correlation energy (E_{xc}^{HSE06}) and the Coulomb potential are partitioned into long range (LR) and short range (SR) terms. 25% exact exchange obtained from Hartree–Fock calculations ($E_x^{Fock,SR}$) is combined with the inexact SR exchange ($E_x^{PBE,SR}$) of DFT, while the DFT LR exchange ($E_x^{PBE,LR}$) and correlation (E_c^{PBE}) are unaffected. Specifically, the general gradient approximation (GGA) of Perdew, Burke, and Ernzerhof (PBE)[56] is utilized here, and the Coulomb potential is partitioned into LR and SR terms using a screening parameter of 0.207 $Å^{-1}$.

$$E_{xc}^{HSE06} = E_x^{HSE06,SR} + E_x^{PBE,LR} + E_c^{PBE} \quad (1)$$

where

$$E_x^{HSE06,SR} = \frac{1}{4}E_x^{Fock,SR} + \frac{3}{4}E_x^{PBE,SR} \quad (2)$$

The long range nature of the Hartree–Fock exchange in both B3LYP and PBE0 incurs substantial computational constraints, while in HSE06, partitioning the exchange–correlation energy into short range and long range terms and only considering short range mixing with Hartree–Fock exchange greatly reduces the computational cost.[53] In addition, HSE06 has been shown to give equivalent and even improved results compared to PBE0 and B3LYP in a number of systems despite performing calculations in a significantly reduced timeframe.[57–59]

Results obtained using the hybrid approach have been shown to be in better agreement with experimental data for structures and band gaps when compared to standard DFT functionals.[60–68] For the purpose of comparison, calculations were also carried out with GGA + U (U_{Cu}^{3d} = 5.2 eV,[69–71]), where the +U correction of Dudarev *et al.*[72] acts as an energetic penalty to the delocalization of states.

Interactions between the core of each atom (Cu:[Ar], Sb:[Kr], Bi:[Xe], S:[Ne], Se:[Ar]) and the valence electrons were described using the projector-augmented wave (PAW) method.[73,74] A plane wave energy cut off of 300 eV and a k-point sampling of 3 × 2 × 3 were used for all systems. A convergence criterion for the residual forces on each atom of 0.01 eV Å^{-1} was employed. VESTA was used to carry out visual and structural analysis of the systems.[75]

For each material, optimization of the atomic positions and lattice vectors was performed, and the resulting energy–volume curves were fitted to the Murnaghan equation of state to obtain the equilibrium bulk cell volume.[76] Electronic density of states (EDOS) and band structure calculations were carried out, with the symmetry labels used in the band structures taken from Bradley and Cracknell.[77] The transversal approximation and PAW method were used to compute the optical transition matrix elements and the optical absorption spectrum.[78] This methodology sums the adsorption spectra over all direct valence band (VB) to conduction band (CB) transitions, and indirect and intraband adsorptions are not considered.[79] Previous studies have shown this single particle transition method to provide reasonable optical absorption spectra,[80–86] despite the electron–hole correlations not being addressed.

3 Results

The lattice parameters for each material, obtained after the structural relaxation, are shown in Table 1. GGA + U is seen to overestimate all of the lattice constants in comparison with experimental values, while HSE06 calculations result in underestimation of some parameters and overestimation of others. The magnitude of the difference between the computational and experimental values is in almost all cases smaller for HSE06 than for GGA + U. Notably, both functionals overestimate the ***a*** lattice vector for all systems relative to experiment, indicating that the lone pairs which are present in this direction are distorting the simulated structures. No experimental data was available for Cu_3BiSe_3, although the volume of the relaxed unit cell was found to be 600.93 Å^3, greater than that of the other cells due to the relative sizes of the constituent atoms.

Table 1 Lattice vectors and volumes for minimum energy structures of the materials (values in parentheses are % difference to experimental values). Lengths are reported in Å and volumes in Å^3

		Expt.[a]	GGA + U	HSE06
Cu_3SbS_3	***a***	7.884	8.162 (3.52)	8.018 (1.70)
	b	10.221	10.291 (0.68)	10.111 (−1.07)
	c	6.624	6.744 (1.80)	6.621 (−0.05)
	V	533.78	566.38 (6.11)	536.78 (0.56)
Cu_3SbSe_3	***a***	7.987	8.092 (1.32)	8.058 (0.89)
	b	10.614	10.730 (1.10)	10.598 (−0.15)
	c	6.837	7.017 (2.63)	6.945 (1.58)
	V	579.57	609.27 (13.00)	593.17 (2.35)
Cu_3BiS_3	***a***	7.723	7.908 (2.39)	7.857 (1.74)
	b	10.395	10.474 (0.76)	10.332 (−0.61)
	c	6.716	6.843 (1.89)	6.847 (1.95)
	V	539.16	566.71 (5.11)	555.86 (3.10)
Cu_3BiSe_3	***a***	—	8.063	8.025
	b	—	10.804	10.652
	c	—	7.093	7.030
	V	—	617.94	600.93

[a] Cu_3SbS_3 (ref. 38), Cu_3SbSe_3 (ref. 40), and Cu_3BiS_3 (ref. 41).

The total and partial (l-decomposed) EDOS of each system has been plotted in Fig. 2 and shows a similar distribution of the electronic states in all fours systems. The lowest energy states shown, labeled as features I and II, are predominantly S/Se and Sb/Bi s states, respectively, with a small amount of anion p-state mixing. The VB, represented by the dense region of states between −6 and 0 eV (features III through V), is mostly comprised of Cu d, Sb/Bi p, and S/Se p states, although there is also a small amount of Sb/Bi s density present. The CB (feature VI) consists almost entirely of both Sb/Bi and S/Se p states, with some minor S/Se s contribution. The Sb/Bi s states are at the bottom of the VB, too low in energy to interact with the Sb/Bi p states.[87] However, through mixing of these s states with the anion p states, a filled antibonding state is produced at the top of the VB where the Sb/Bi s states can mix with the Sb/Bi p states.[88,89] This results in lone pair states on the Sb and Bi ions, as evidenced by the anisotropic charge distribution surrounding these atoms in the charge density plots in Fig. 3. The square of the absorption coefficient as a function of photon energy is plotted in Fig. 4 for all four systems. The direct, optical band gaps for Cu_3SbS_3, Cu_3BiS_3, Cu_3SbSe_3, and Cu_3BiSe_3, as calculated by HSE06, are 2.13 eV, 1.76 eV, 1.79 eV, and 1.43 eV, respectively. Cu_3SbSe_3, Cu_3BiS_3 and Cu_3BiSe_3 have optical band gaps within the optimal range, with Cu_3BiSe_3 having the closest optical band gap to the optimum value of 1.5 eV.

As seen in the band structures (Fig. 5), all the materials studied showed an indirect fundamental band gap from the VBM at Γ to the conduction band minimum (CBM) at U. The fundamental band gaps of Cu_3SbS_3, Cu_3SbSe_3, Cu_3BiS_3, and Cu_3BiSe_3 were calculated by HSE06 to be 2.02 eV, 1.50 eV, 1.69 eV,

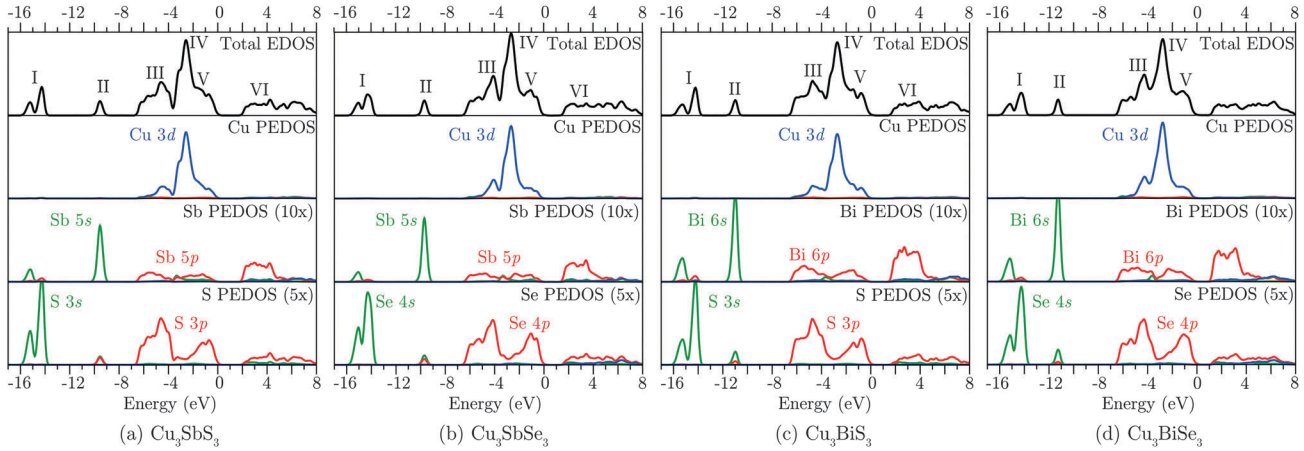

Fig. 2 Total and partial electronic density of states (with appropriate scaling) (a) Cu_3SbS_3, (b) Cu_3SbSe_3, (c) Cu_3BiS_3, and (d) Cu_3BiSe_3 as calculated with HSE06. The valence band maximum (VBM) has been set to 0 eV.

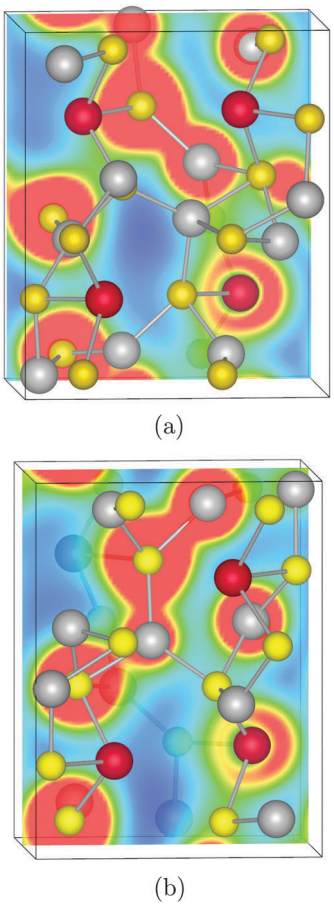

Fig. 3 Charge density plots of (a) Cu_3SbS_3 and (b) Cu_3BiS_3. Cu ions are shown as gray, Sb/Bi ions as red, and S/Se ions as yellow. The electron density is shown at 0.05 eV Å^{-3}.

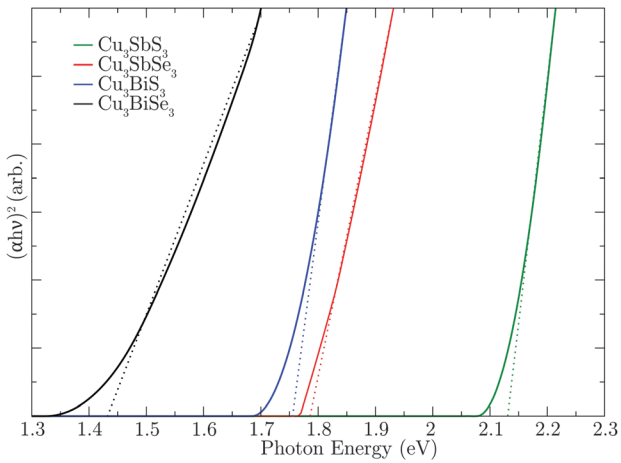

Fig. 4 The absorption coefficient squared (α^2) *versus* photon energy (eV) for each material. Linear regression (shown as dotted lines) is used to determine the optical band gap.

and 1.17 eV, respectively, as shown in Table 2. However, optical analysis performed with HSE06 reveals that the onset of direct optical absorption in each of the materials is from the highest valence band to the lowest conduction band at the Γ point.

Estimation of the effective mass at the band edges shows that for each of the materials, the lowest effective mass is in the Γ–X direction for the VB and in the U–Z direction for the CB (Table 3). The magnitude of the effective mass indicates a dependence on whether the material is a sulphide or a selenide, with the latter displaying lower hole and electron effective masses than the former. That the nature of the anion has a significant effect on the effective masses is consistent with the density of anion p states at the both the VBM and CBM, as seen in the EDOS (Fig. 2). Cu_3BiS_3 has an experimentally determined effective hole mass of 0.35 m_e,[46] which is in good agreement with our calculated value of 0.432 m_e. The small discrepancy with the calculated value may be as a result of the calculation not accounting for spin–orbit coupling, a notable factor when describing the curvature of bands of systems with heavy atoms such as Bi.[90,91] To check this, GGA + U band structure calculations with and without spin–orbit coupling were performed for Cu_3BiS_3 and Cu_3BiSe_3, giving effective hole masses of 0.477 m_e for Cu_3BiS_3 and 0.249 m_e for Cu_3BiSe_3 along the Γ–X direction

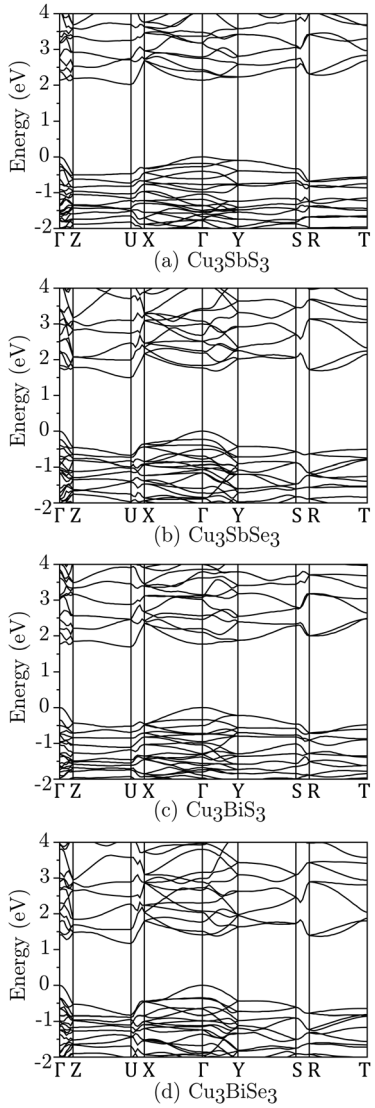

Fig. 5 Band structures of (a) Cu_3SbS_3, (b) Cu_3SbSe_3, (c) Cu_3BiS_3, and (d) Cu_3BiSe_3, calculated with HSE06. In each case the VBM has been set to 0 eV.

with the spin–orbit coupling, compared to 0.432 m_e for Cu_3BiS_3 and 0.230 m_e for Cu_3BiSe_3 without. The inclusion of a spin–orbit term results in a slight increase in the hole effective mass of both systems, indicating that the calculations without spin–orbit coupling are reasonable. For all materials, the overall effective mass in the VB is lower than that of the CB, suggesting that these materials will display better hole mobility than electron mobility, in agreement with experimental evidence that they are p-type.[43,44]

Table 3 The calculated effective mass of carriers in the VB and CB

	Valence band (m_e)			Conduction band (m_e)	
	$\Gamma \rightarrow X$	$\Gamma \rightarrow Y$	$\Gamma \rightarrow Z$	$U \rightarrow X$	$U \rightarrow Z$
Cu_3SbS_3	0.453	1.471	1.196	0.779	0.505
Cu_3SbSe_3	0.245	0.902	1.112	0.554	0.378
Cu_3BiS_3	0.432	1.286	1.481	0.679	0.522
Cu_3BiSe_3	0.256	1.037	1.045	0.526	0.312

4 Discussion

As seen from the EDOS, while the Sb/Bi valence s states contribute mainly to a large peak at around 10 eV below the VBM, they also provide a small amount of density in the VB. This is due to the lone pair effect associated with the heavy metals in groups 13–16, for which there are two stable oxidation states (the group valency n and $n - 2$) as a result of mixing between the ns electrons and the np electrons. However, although classical lone pair theory is based on the direct mixing of these two states, the metal s states are generally too far in energy below the VB to interact with the metal p states, as has been shown by a number of computational studies and confirmed by experiment.[92–95] The rationale behind the mixing of the Sb/Bi s and the p states in spite of the energy difference is a result of the revised lone pair theory.[87]

In agreement with this model, the Sb/Bi s states mix with some anion p density at around −10 eV (relative to the VBM), creating a filled antibonding state at the VBM. This accounts for the minor Sb/Bi s state contribution to the VB, where it can interact with the unfilled Sb/Bi p states in the CB to create the lone pair effect. As group 16 p states increase in energy down the group, the p states of S have a greater interaction with the cation s states than those of Se. Therefore, the lone pair mixing is most in evidence in the sulphides.[87,93] For lone pair dependence on metal variation, relativistic effects on the core electrons in Bi lower the energy of the 6s states, thereby increasing the gap between the 6s and p states and reducing the lone pair effect relative to the Sb chalcogenides.[87] Therefore, lone pairs have the greatest influence in Cu_3SbS_3 and the least in Cu_3BiSe_3.

It is important that a good absorber material possesses adequate conductivity, a band gap within the optimal range, and the ability to readily absorb photons. Cu_3SbS_3 has a band gap greater than the viable window of 0.9 eV to 1.8 eV,[96]

Table 2 Results for both the GGA + U and HSE06 calculations of the direct (E_g^d) and indirect (E_g^i) band gaps of $CuMCh_3$ (M = Sb, Bi; Ch = S, Se). Linear regression (denoted by the dotted lines) of the optical absorption in Fig. 4 was used to estimate the optical band gaps (E_g^o). Experimental values are listed for comparison, with (d) and (i) denoting reported direct and indirect optical band gaps, respectively

	E_g^d(GGA + U)	E_g^d(HSE06)	E_g^i(GGA + U)	E_g^i(HSE06)	E_g^o(GGA + U)	E_g^o(HSE06)	$E_g^{expt.}$
Cu_3SbS_3	1.33	2.14	1.22	2.02	1.61	2.13	2.95 (i)[48]
Cu_3SbSe_3	1.11	1.77	0.89	1.50	1.37	1.76	1.68 (d)[49]
Cu_3BiS_3	1.15	1.77	1.09	1.69	1.59	1.79	1.4 (d)[44]
Cu_3BiSe_3	0.94	1.41	0.68	1.17	1.21	1.43	—

making it immediately unappealing as an absorber material. Our HSE06 calculated band gap for Cu_3SbS_3 is *significantly* underestimated compared to the only recorded experimental value of 2.95 eV.[48] However, the previously reported value was for the Skinnerite structure, whereas we have studied the material in its low temperature phase, and additionally, the particles studied were nanorods so it is reasonable that the band gap was potentially subject to quantum confinement effects. Regardless, even the value obtained from our calculations is considered too high for potential solar cell application.

Examining the fundamental indirect band gaps of the other systems, all three fall within the acceptable range. Cu_3SbSe_3 has a predicted optical band gap greater than the observed optical band gap of 1.68 eV,[49] perhaps due to HSE06 overestimating the band gap, a tendency of the functional that has been previously observed.[97,98] Analysis of the direct, allowed optical transitions from VB to CB for Cu_3BiS_3 indicates that there exists a direct, allowed absorbance at an energy equal to the difference in the eigenvalues of the VB and CB at the Γ point, contrary to the experimental result of the absorbance being a direct, forbidden transition;[44] the optical band gap is also overestimated with respect to the experimental value of 1.4 eV.[44] Of the four materials, Cu_3BiSe_3 has the closest optical band gap to the optimum band gap of 1.5 eV for PV devices.[2]

For all the materials studied, the overall effective mass of the VB is lower than that of the CB, suggesting that these materials are likely to display hole mobility over electron mobility, which is consistent with experimental evidence that these materials are p-type in nature.[43,44] Despite the indirect nature of their band gaps (meaning that the lowest electronic transitions must be phonon-assisted and hence lowering the PV efficiency of the material[99]), Cu_3BiS_3, Cu_3SbSe_3, and Cu_3BiS_3 all possess optical band within the optimum spectral range for PV absorbers. The difference between the fundamental indirect band gaps and the optical band gaps is small in all three cases, meaning that these materials should be more efficient than c-Si absorbers and should still be suitable for thin film PV applications. To truly understand the conductivity of this material, however, a full defect analysis of this system and valence band alignment would need to be undertaken and, in light of the promising results reported herein, is certainly warranted.

5 Conclusions

The geometry, electronic structure, and optical properties of Cu_3MCh_3 (M = Sb, Bi; Ch = S, Se) were investigated using screened hybrid DFT, and the materials' suitability as potential absorber layers for PV devices was assessed. All materials were shown to possess reasonably low effective masses at the VBM, and lower VBM effective masses compared to CBM effective masses, with the increased curvature at the VBM clearly influenced by the lone pair effects on Sb and Bi. The fundamental band gaps of all four materials are indirect in nature, but their optical band gaps are very close in energy, with the optical band gaps of Cu_3SbSe_3 (1.76 eV), Cu_3BiS_3 (1.79 eV), and Cu_3BiSe_3 (1.43 eV) being within the accepted spectral range for PV absorbers. Therefore, Cu_3SbSe_3, Cu_3BiS_3, and Cu_3BiSe_3 warrant further investigation as alternative solar cell absorber materials.

Acknowledgements

This research was supported by SFI through the PI programme (PI Grant numbers 06/IN.1/I92 and 06/IN.1/I92/EC07). Calculations were performed on the Lonsdale cluster maintained by TCHPC. D. O. S. is grateful to the Ramsay Memorial Trust and University College London for a Ramsay Fellowship. A. B. K. and D. J. T. would like to thank the Irish Research Council for the provision of postgraduate scholarships.

References

1 A. Shah, P. Torres, R. Tscharner, N. Wyrsch and H. Keppner, *Science*, 1999, **285**, 692–698.
2 K. L. Chopra, P. D. Paulson and V. Dutta, *Prog. Photovoltaics*, 2004, **12**, 69–92.
3 M. A. Contreras, K. Ramanathan, J. AbuShama, F. Hasoon, D. L. Young, B. Egaas and R. Noufi, *Prog. Photovoltaics*, 2005, **13**, 209–216.
4 S. B. Zhang, S. H. Wei, A. Zunger and H. Katayama-Yoshida, *Phys. Rev. B: Condens. Matter Mater. Phys.*, 1998, **57**, 9642–9656.
5 C. Persson, Y.-J. Zhao, S. Lany and A. Zunger, *Phys. Rev. B: Condens. Matter Mater. Phys.*, 2005, **72**, 035211.
6 W. J. Jeong and G. C. Park, *Sol. Energy Mater. Sol. Cells*, 2003, **75**, 93–100.
7 First Solar, First Solar sets world record for CdTe solar PV efficiency, 2011, http://investor.firstsolar.com/releasedetail.cfm?ReleaseID=593994.
8 P. Jackson, D. Hariskos, E. Lotter, S. Paetel, R. Wuerz, R. Menner, W. Wischmann and M. Powalla, *Prog. Photovoltaics*, 2011, **19**, 894–897.
9 B. A. Anderson, *Prog. Photovoltaics*, 2000, **8**, 61–76.
10 H. Matsushita, T. Maeda, A. Katsui and T. Takizawa, *J. Cryst. Growth*, 2000, **208**, 416–422.
11 T. K. Todorov, K. B. Reuter and D. B. Mitzi, *Adv. Mater.*, 2010, **22**, E156–E159.
12 D. O. Scanlon and A. Walsh, *Appl. Phys. Lett.*, 2012, **100**, 251911.
13 T. Watkins, A. V. G. Chizmeshya, L. Y. Jiang, D. J. Smith, R. T. Beeler, G. Grzybowski, C. D. Poweleit, J. Menendez and J. Kouvetakis, *J. Am. Chem. Soc.*, 2011, **133**, 16212–16218.
14 J.-H. Yang, Y. Zhai, H. Liu, H. Xiang, X. Gong and S.-H. Wei, *J. Am. Chem. Soc.*, 2012, **134**, 12653–12657.
15 F. J. Disalvo, *Science*, 1990, **247**, 649–655.
16 H. Nakanishi, S. Endo and I. Taizo, *Jpn. J. Appl. Phys.*, 1969, **8**, 443.
17 J. Li and H. Y. Guo, *J. Solid State Chem.*, 1995, **117**, 247–255.
18 R. W. Miles, G. Zoppi and I. Forbes, *Mater. Today*, 2007, **10**, 20–27.
19 E. J. Skoug, J. D. Cain and D. T. Morelli, *Appl. Phys. Lett.*, 2010, **96**, 181905.
20 D. J. Temple, A. B. Kehoe, J. P. Allen, G. W. Watson and D. O. Scanlon, *J. Phys. Chem. C*, 2012, **116**, 7334–7340.
21 H. Katagiri, *Thin Solid Films*, 2005, **480**, 426–432.

22 S. Y. Chen, A. Walsh, J. H. Yang, X. G. Gong, L. Sun, P. X. Yang, J. H. Chu and S. H. Wei, *Phys. Rev. B: Condens. Matter Mater. Phys.*, 2011, **83**, 125201.
23 S. Bag, O. Gunawan, T. Gokmen, Y. Zhu, T. K. Todorov and D. B. Mitzi, *Energy Environ. Sci.*, 2012, **5**, 7060–7065.
24 J. J. Scragg, P. J. Dale, L. M. Peter, G. Zoppi and I. Forbes, *Phys. Status Solidi B*, 2008, **245**, 1772–1778.
25 N. Kamoun, H. Bouzouita and B. Rezig, *Thin Solid Films*, 2007, **515**, 5949–5952.
26 R. A. Wibowo, W. S. Kim, E. S. Lee, B. Munir and K. H. Kim, *J. Phys. Chem. Solids*, 2007, **68**, 1908–1913.
27 S. C. Riha, B. A. Parkinson and A. L. Prieto, *J. Am. Chem. Soc.*, 2011, **133**, 15272–15275.
28 J. Ma, Y. Wang, Y. Wang, P. Peng, J. Lian, X. Duan, Z. Liu, X. Liu, Q. Chen, T. Kim, G. Yao and W. Zheng, *CrystEngComm*, 2011, **13**, 2369–2374.
29 R. Vadapoo, S. Krishnan, H. Yilmaz and C. Marin, *Phys. Status Solidi B*, 2011, **248**, 700–705.
30 S. A. Manolache, M. Nanu, A. Dută, A. Goossens and J. Schoonman, Semiconductor Conference, 2005. CAS 2005 Proceedings. 2005 International, 2005, pp. 145–148.
31 D. Li and X. Y. Qin, *J. Appl. Phys.*, 2006, **100**, 023713.
32 *US Geological Survey, Mineral commodity summaries 2012*, United States Government Printing Office, Washington, DC, 2012.
33 *US Geological Survey, Mineral commodity summaries 2008*, United States Government Printing Office, Washington, DC, 2008.
34 *US Geological Survey, Mineral commodity summaries 2007*, United States Government Printing Office, Washington, DC, 2007.
35 *US Geological Survey, Mineral commodity summaries 2011*, United States Government Printing Office, Washington, DC, 2011.
36 L. Yu, R. S. Kokenyesi, D. A. Keszler and A. Zunger, *Adv. Energy Mater.*, 2013, **3**, 43–48.
37 H. J. Whitfield, *Solid State Commun.*, 1980, **33**, 747–748.
38 A. Pfitzner, *Z. Kristallogr.*, 1998, **213**, 228–236.
39 E. Makovicky and T. Bailć-Žunić, *Can. Mineral.*, 1995, **33**, 655–663.
40 A. Pfitzner, *Z. Anorg. Allg. Chem.*, 1995, **621**, 685–688.
41 V. Kocman and E. Nuffield, *Acta Crystallogr., Sect. B: Struct. Sci.*, 1973, **29**, 2528–2536.
42 H. Hu, O. Gomez-Daza and P. K. Nair, *J. Mater. Res.*, 1998, **13**, 2453–2456.
43 V. Estrella, M. T. S. Nair and P. K. Nair, *Semicond. Sci. Technol.*, 2003, **18**, 190–194.
44 N. J. Gerein and J. A. Haber, *Chem. Mater.*, 2006, **18**, 6297–6302.
45 F. Mesa, A. Dussan and G. Gordillo, *Phys. B.*, 2009, **404**, 5227–5230.
46 F. Mesa, G. Gordillo, T. Dittrich, K. Ellmer, R. Baier and S. Sadewasser, *Appl. Phys. Lett.*, 2010, **96**, 082113.
47 Z. Jiasong, X. Weidong, J. Huaidong, C. Wen, L. Lijun, Y. Xinyu, L. Xioajuan and L. Haitao, *Mater. Lett.*, 2010, **64**, 1499–1502.
48 M. X. Wang, G. H. Yue, X. Y. Fan and P. X. Fan, *J. Cryst. Growth*, 2008, **310**, 3062–3066.
49 A. M. Fernandez and J. A. Turner, *Sol. Energy Mater. Sol. Cells*, 2003, **79**, 391–399.
50 N. B. Babanly, Y. A. Yusibov, Z. S. Aliev and M. B. Babanly, *Russ. J. Inorg. Chem.*, 2010, **55**, 1471–1481.
51 G. Kresse and J. Hafner, *Phys. Rev. B: Condens. Matter Mater. Phys.*, 1994, **49**, 14251–14271.
52 G. Kresse and J. Furthmüller, *Phys. Rev. B: Condens. Matter Mater. Phys.*, 1996, **54**, 11169–11186.
53 S. Heyd, G. E. Scuseria and M. Ernzerhof, *J. Chem. Phys.*, 2003, **118**, 8207–8215.
54 A. D. Becke, *J. Chem. Phys.*, 1993, **98**, 5648–5652.
55 C. Adamo and V. Barone, *J. Chem. Phys.*, 1999, **110**, 6158–6170.
56 J. P. Perdew, K. Burke and M. Ernzerhof, *Phys. Rev. Lett.*, 1996, **77**, 3865–3868.
57 B. G. Janesko, T. M. Henderson and G. E. Scuseria, *Phys. Chem. Chem. Phys.*, 2009, **11**, 443–454.
58 T. M. Henderson, J. Paier and G. E. Scuseria, *Phys. Status Solidi B*, 2011, **248**, 767–774.
59 E. N. Brothers, A. F. Izmaylov, J. O. Normand, V. Barone and G. E. Scuseria, *J. Chem. Phys.*, 2008, **129**, 011102.
60 J. P. Allen, D. O. Scanlon and G. W. Watson, *Phys. Rev. B: Condens. Matter Mater. Phys.*, 2010, **81**, 161103(R).
61 D. O. Scanlon and G. W. Watson, *J. Phys. Chem. Lett.*, 2010, **1**, 2582–2585.
62 B. G. Janesko, T. M. Henderson and G. E. Scuseria, *Phys. Chem. Chem. Phys.*, 2009, **11**, 443–454.
63 D. O. Scanlon, B. J. Morgan, G. W. Watson and A. Walsh, *Phys. Rev. Lett.*, 2009, **103**, 096405.
64 A. B. Kehoe, D. O. Scanlon and G. W. Watson, *Phys. Rev. B: Condens. Matter Mater. Phys.*, 2011, **83**, 233202.
65 J. L. F. Da Silva, M. V. Ganduglia-Pirovano, J. Sauer, V. Bayer and G. Kresse, *Phys. Rev. B: Condens. Matter Mater. Phys.*, 2007, **75**, 045121.
66 D. O. Scanlon, A. B. Kehoe, G. W. Watson, M. O. Jones, W. I. F. David, D. J. Payne, R. G. Egdell, P. P. Edwards and A. Walsh, *Phys. Rev. Lett.*, 2011, **107**, 246402.
67 J. Heyd and G. E. Scuseria, *J. Chem. Phys.*, 2004, **121**, 1187–1192.
68 M. Burbano, D. O. Scanlon and G. W. Watson, *J. Am. Chem. Soc.*, 2011, **133**, 15065–15072.
69 D. O. Scanlon, A. Walsh, B. J. Morgan, D. Payne, R. G. Egdell and G. W. Watson, *Phys. Rev. B: Condens. Matter Mater. Phys.*, 2009, **79**, 035101.
70 T. Arnold, D. J. Payne, A. Bourlange, J. P. Hu, R. G. Egdell, L. F. J. Piper, L. Colakerol, A. Masi, P. A. Glans, T. Learmonth, K. E. Smith, J. Guo, D. O. Scanlon, A. Walsh, B. J. Morgan and G. W. Watson, *Phys. Rev. B: Condens. Matter Mater. Phys.*, 2009, **79**, 075102.
71 K. G. Godinho, B. J. Morgan, J. P. Allen, D. O. Scanlon and G. W. Watson, *J. Phys.: Condens. Matter*, 2011, **23**, 334201.
72 S. L. Dudarev, G. A. Botton, S. Y. Savrasov, C. J. Humphreys and A. P. Sutton, *Phys. Rev. B: Condens. Matter Mater. Phys.*, 1998, **57**, 1505–1509.

73 P. E. Blöchl, *Phys. Rev. B: Condens. Matter Mater. Phys.*, 1994, **50**, 17953–17979.
74 G. Kresse and D. Joubert, *Phys. Rev. B: Condens. Matter Mater. Phys.*, 1999, **59**, 1758–1775.
75 K. Momma and F. Izumi, *J. Appl. Crystallogr.*, 2008, **41**, 653–658.
76 F. D. Murnaghan, *Proc. Natl. Acad. Sci. U. S. A.*, 1944, **30**, 244–247.
77 C. J. Bradley and A. P. Cracknell, *Mathematical Theory of Symmetry in Solids*, Oxford Univeristy Press, Ely House, London W.1, 1972.
78 M. Gajdos, K. Hummer, G. Kresse, J. Furthmuller and F. Bechstedt, *Phys. Rev. B: Condens. Matter Mater. Phys.*, 2006, **73**, 045112.
79 B. Adolph, J. Furthmuller and F. Beckstedt, *Phys. Rev. B: Condens. Matter Mater. Phys.*, 2001, **63**, 125108.
80 X. Nie, S. H. Wei and S. B. Zhang, *Phys. Rev. Lett.*, 2002, **88**, 066405.
81 A. Walsh, Y. Yan, M. N. Huda, M. M. Al-Jassim and S. H. Wei, *Chem. Mater.*, 2009, **21**, 547–551.
82 D. O. Scanlon and G. W. Watson, *Chem. Mater.*, 2009, **21**, 5435–5442.
83 J. P. Allen, D. O. Scanlon and G. W. Watson, *Phys. Rev. B: Condens. Matter Mater. Phys.*, 2011, **84**, 115141.
84 K. G. Godinho, J. J. Carey, B. J. Morgan, D. O. Scanlon and G. W. Watson, *J. Mater. Chem.*, 2010, **20**, 1086–1096.
85 D. O. Scanlon, A. Walsh and G. W. Watson, *Chem. Mater.*, 2009, **21**, 4568–4576.
86 J. P. Allen, M. K. Nilsson, D. O. Scanlon and G. W. Watson, *Phys. Rev. B: Condens. Matter Mater. Phys.*, 2011, **83**, 035207.
87 A. Walsh, D. J. Payne, R. G. Egdell and G. W. Watson, *Chem. Soc. Rev.*, 2011, **40**, 4455–4463.
88 A. Walsh, G. W. Watson, D. J. Payne, R. G. Edgell, J. H. Guo, P. A. Glans, T. Learmonth and K. E. Smith, *Phys. Rev. B: Condens. Matter Mater. Phys.*, 2006, **73**, 235104.
89 J. P. Allen, J. J. Carey, A. Walsh, D. O. Scanlon and G. W. Watson, *J. Phys. Chem. C*, 2013, **117**, 14759–14769, DOI: 10.1021/jp4026249.
90 D. Parker and D. J. Singh, *Phys. Rev. B: Condens. Matter Mater. Phys.*, 2011, **83**, 233206.
91 D. O. Scanlon, P. D. C. King, R. P. Singh, A. de la Torre, S. M. Walker, G. Balakrishnan, F. Baumberger and C. R. A. Catlow, *Adv. Mater.*, 2012, **24**, 2154–2158.
92 G. W. Watson, *J. Chem. Phys.*, 2001, **114**, 758–763.
93 A. Walsh and G. W. Watson, *J. Phys. Chem. B*, 2005, **109**, 18868–18875.
94 A. Walsh and G. W. Watson, *J. Solid State Chem.*, 2005, **178**, 1422–1428.
95 D. J. Payne, R. G. Egdell, A. Walsh, G. W. Watson, J. H. Guo, P. A. Glans, T. Learmonth and K. E. Smith, *Phys. Rev. Lett.*, 2006, **96**, 157403.
96 A. Nunez, P. K. Nair and M. T. S. Nair, *Mod. Phys. Lett. B*, 2001, **15**, 605–608.
97 D. O. Scanlon and G. W. Watson, *J. Mater. Chem.*, 2011, **21**, 3655–3663.
98 D. O. Scanlon and G. W. Watson, *Phys. Chem. Chem. Phys.*, 2011, **13**, 9667–9675.
99 R. W. Brander, *Rev. Phys. Technol.*, 1972, **21**, 145–194.

